PROCEEDINGS OF SCIENCE

A multiwavelength perspective on the modified LIMA model for CAL 83

A. Odendaal*
University of the Free State, South Africa
E-mail: WinkA@ufs.ac.za

P. J. Meintjes†
University of the Free State, South Africa
E-mail: MeintjPJ@ufs.ac.za

The defining characteristics of supersoft X-ray sources are their very low effective X-ray temperatures, typically $kT_{\rm eff} \sim 20$ -100 eV, together with the extremely high X-ray luminosities, ranging from $\sim 10^{36}$ erg s^{-1} to as high as $\sim 10^{38}$ erg s^{-1}. Previous authors have shown that the supersoft X-ray radiation can be explained by the nuclear burning of hydrogen on the surface of an accreting white dwarf. CAL 83 was one of the first close binary supersoft X-ray sources to be discovered, and exhibits multiwavelength variability on various time-scales, including a peculiar $\sim$67 s X-ray periodicity. In this paper, this X-ray periodicity is compared with the dwarf nova oscillations (DNOs) observed in dwarf novae during outburst, and is found to have very similar properties. It is proposed that the $\sim$67 s periodicity can be satisfactorily explained by an adaptation of the low-inertia magnetic accretor (LIMA) model that has previously been applied to DNOs. In this model, the $\sim$67 s modulation originates in an equatorial belt in the envelope at the boundary with the inner accretion disc, with the belt weakly coupled to the white dwarf core by a $\sim 10^5$ G magnetic field. The quasi-periodic optical modulations on time-scales of several minutes that are observed in CAL 83, are also compatible with this framework. Reconnection events resulting from the winding up of magnetic field lines in the belt may also cause particle acceleration, which can be expected to lead to transient non-thermal emission from radio to gamma-ray energies. This provides very interesting possibilities of observing CAL 83 with next generation telescopes like *MeerKAT* and the SKA at low energies, as well as e.g. *ASTROSAT* at high energies.

3rd Annual Conference on High Energy Astrophysics in Southern Africa - HEASA2015,
18-20 June 2015
University of Johannesburg, Auckland Park, South Africa

*Based on observations obtained with XMM-Newton, an ESA science mission with instruments and contributions directly funded by ESA Member States and NASA, as well as observations with SHOC (Sutherland High-speed Optical Camera) on the SAAO (South African Astronomical Observatory) 1.9-m Telescope at Sutherland.

†Speaker.

PoS(HEASA2015)025

1. Introduction

Supersoft X-ray sources (SSSs) were only established as a distinct class of objects after observations by the *Einstein Observatory* [1, 2] and *ROSAT* [3]. Their defining characteristics are their very low effective X-ray temperatures, typically $kT_{\rm eff} \sim 20$ -100 eV, together with the extremely high X-ray luminosities, ranging from $\sim 10^{36}$ erg s^{-1} to as high as the Eddington limit of $\sim 10^{38}$ erg s^{-1}. The vast majority of observed SSSs are binary systems. It has been shown that the X-ray properties can be explained by steady nuclear burning of accreted hydrogen on the surface of a white dwarf (WD) [4]. To sustain persistent hydrogen nuclear burning on the WD surface, the accretion rate needs to be of the order of $\dot{m}_{\rm acc} \sim 10^{-7}$ M$_\odot$ yr^{-1}.

One of the first discovered SSSs was CAL 83, thus named because it was source number 83 in the Columbia Astrophysics Laboratory survey of the Large Magellanic Cloud (LMC), using the Imaging Proportional Counter (IPC) aboard the *Einstein Observatory* [1, 5]. It was the brightest X-ray point source discovered in this survey that was not associated with a Galactic foreground star or a background AGN (active galactic nucleus). CAL 83 forms part of the so-called "close binary supersoft sources", with its relatively short orbital period of 1.047529 ± 0.000001 d [6]. Spectral fits to *Chandra* and *XMM-Newton* X-ray data indicate a WD primary with $M_{\rm wd} \sim 1.3$ M$_\odot$ and luminosity $L \sim 3.4 \times 10^{37}$ erg s^{-1} [7]. It is often considered the "prototype" of the SSS class, and was originally thought to be a constant X-ray source. However, since its discovery, this system has been found to exhibit intriguing and often unexpected characteristics. A review of its properties is provided by [8], while [9] considered variability in CAL 83.

Close binary supersoft sources have a class of close cousins in the WD binary population, namely the cataclysmic variables (CVs). In CVs, the WD is more massive than the donor. However, it has been shown [4] that the high accretion rate required to drive persistent surface nuclear burning in SSSs is only possible if the donor is more massive than the WD. The main characteristics of SSSs distinguishing them from CVs are therefore their inverted mass ratios, high accretion rates and extreme luminosities derived from surface nuclear burning.

It is well known that CVs exhibit (often dramatic) variability on various time-scales in the optical to X-ray wavebands. Random optical variability on time-scales of seconds to hours is observed in many CVs, known as "flickering" [10]. Many CVs also exhibit variability with a preferred time-scale, but not strictly periodic. These quasi-periodic modulations have periods between a few seconds and a few thousand seconds, and can be broadly classified into the following groups: dwarf nova oscillations (DNOs), longer period DNOs (lpDNOs) and quasi-periodic oscillations (QPOs) (see e.g. the review papers of [11] and [12] for details). These types of modulations have been very well studied in CVs, but because of the great similarity between CVs and supersoft X-ray binaries, similar quasi-coherent signals can be expected from the latter class of objects.

In fact, a recently discovered X-ray modulation at $\sim$67 s in CAL 83 [13] bears a remarkable resemblance to DNOs (see also the independent remarks of [14]). The favoured interpretation for DNOs is that they originate from a region close to the surface of a WD with a magnetic field too weak to enable rigid body rotation of the core and exterior region, but strong enough to control accretion close to its surface. This is known as the low-inertia magnetic accretor (LIMA) model ([15] and references therein).

In this paper, the application of a similar LIMA model on the $\sim$67 s periodicity in CAL 83 is

discussed, and also the implications of the presence of weakly magnetized accreted material on the WD surface in terms of potential transient high energy emission (hard X-ray en soft gamma-ray). In §2, the known broadband multiwavelength variability of CAL 83 is discussed, in order to provide context for the rest of the paper. A review of the properties of the ∼67 s periodicity is provided in §3. This is followed by a summary of the existing LIMA model for DNOs in §4, and a discussion of the application of an adapted LIMA model on CAL 83 in §5. In supplementation of the X-ray results, optical lightcurves of CAL 83 are presented in §6, as obtained with the Sutherland High-speed Optical Camera (SHOC) on the SAAO[1] 1.9-m Telescope at Sutherland. In §7, potential transient non-thermal emission is discussed, followed by the conclusion in §8.

2. Summary of broadband multiwavelength variability in CAL 83

In addition to orbital modulations with amplitude ∼0.1 mag, the optical lightcurves also exhibit pronounced brightness changes with an amplitude of ∼1 mag. These modulations are quasi-periodic with a period of ∼450 d [6]. Since its discovery, CAL 83 has been observed 8 times during X-ray off-states, coinciding with optical high states. In fact, higher X-ray luminosities are consistently associated with lower optical luminosities. New results on this anti-correlated behaviour were presented by [6], as well as a review of previously published results. The X-ray luminosity during on-states is also variable on time-scales of minutes, and it has been shown that higher X-ray luminosities are associated with higher effective X-ray temperatures [16, Chapter 4].

This anti-correlation between X-ray and optical flux has been explained by so-called "limit cycle" models involving changes in $\dot{m}_{\rm acc}$. A small increase in $\dot{m}_{\rm acc}$ causes excess material to pile up, increasing the WD photospheric radius, as well as the irradiation of the accretion disc and the rate of inward flow through the disc. The shift of the WD spectrum towards longer wavelengths, as well as the increased irradiation and resulting emission of reprocessed radiation from the disc (and the disc wind?) will cause a decrease in the X-ray luminosity and an increase in the optical luminosity (also see [17] and references therein). Once the excess material has been drained, or the mass transfer rate from the secondary decreases, the contraction in the WD photosphere shifts the emission peak to soft X-rays again.

A periodicity of ∼38.4 min was discovered in the single *Chandra* lightcurve that was obtained during an X-ray on-state [18]. This was ascribed to non-radial pulsations of the accreting WD. Several *XMM-Newton* observations of CAL 83 also seem to exhibit similar X-ray quasi-periodicities in the range of ∼10 min to a few hours [9].

3. Review of the ∼67 s periodicity

There are 23 observations of CAL 83 in the *XMM-Newton* Science Archive: 1 obtained in 2000, 5 in 2007, 16 in 2008 and 1 in 2009. Among these, 4 were performed during an X-ray off-state. The 19 on-state observations can be separated into 2 groups, with 8 X-ray "bright" states where the EPIC pn count rate was > 5 counts s^{-1}, and 11 X-ray "faint" states with an EPIC count rate < 2 counts s^{-1}. The lengths of the observations ranged from ∼6 to ∼46 ks. After a systematic

[1] South African Astronomical Observatory

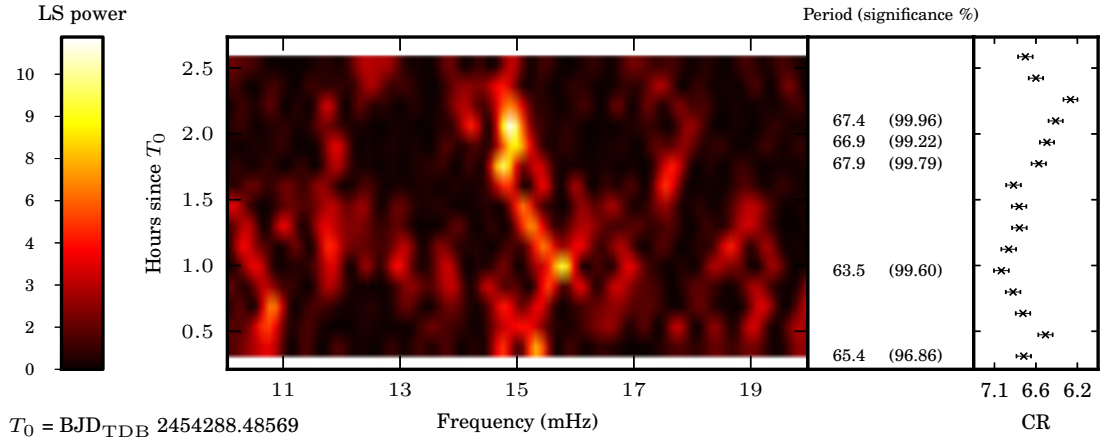

Figure 1: Dynamic LS periodogram of the EPIC pn data of observation 0500860301 of CAL 83, illustrating the variability in the value of $P(\sim 67$ s). The colour represents the LS power, and if a peak was detected between 13.5 and 16.5 mHz at a >95.45% significance level, the corresponding period in seconds and its significance percentage are given. The error in the period values is ± 1 s. The BJD$_{\rm TDB}$ reference represents the start of the observation. The broadband (0.15-1 keV) EPIC pn count rate (CR) is also plotted.

Lomb-Scargle (LS) analysis of all these observations, the discovery of a period with a mean value of $\sim$67 s (hereafter $P(\sim 67$ s)) was reported in the periodograms of all the X-ray bright observations, and also in the X-ray faint observation with the highest count rate[2] [13]. $P(\sim 67$ s) for the different observations varied by up to $\sim$3 s from the mean value. Modulation semi-amplitudes in the 2.5-8.6% range were determined for $P(\sim 67$ s).

To investigate this variability, each observation was subdivided into shorter segments, each 2245 s long, with the centre of each segment displaced by $\sim$600 s in time relative to the centre of the previous one. An LS analysis (using the Starlink PERIOD package) was performed for each segment, yielding for each observation a series of periodograms in the form of a moving average. As an example, such a dynamic periodogram is shown in Fig. 1 for observation 0500860301 on 6 July 2007. For each segment, the strongest peak between 13.5 mHz (74.1 s) and 16.5 mHz (60.6 s) was identified, and its corresponding period and significance level over white noise are also given *if* the peak significance is >95.45%. The variability of the peak on quite short time-scales is obvious. The dynamic periodograms of the other observations exhibited similar behaviour.

The degree of coherence of a periodicity P is often described by $Q = |dP/dt|^{-1}$, i.e. fast changes in the period yield a small Q. For the coherent WD spin period in the intermediate polar DQ Her, $Q \sim 10^{12}$ (e.g. [19]). The value of Q for $P(\sim 67$ s) was calculated from the two longest observations (0500860601 and 0506531701), and was typically a few times 10^2. The rotation period P_* of the WD in CAL 83 is not known, but the low coherence of $P(\sim 67$ s) contradicts its direct association with P_*.

[2]The non-detection of the peak in the other faint observations may simply imply that the signal was too low for the periodicity to be detected, and not necessarily that the periodicity was inherently absent at these epochs.

4. Dwarf nova oscillations and the LIMA model

Dwarf nova oscillations (DNOs) are observed in dwarf novae (DNe) during outburst, and also in other CVs with high accretion rates, but are noticeably absent in almost all intermediate polars (e.g. [12]). (In this context, a "high" $\dot{m}_{\rm acc}$ does not necessarily refer to the very high $\dot{m}_{\rm acc}$ needed for steady nuclear burning, but just higher than that of DNe during quiescence, i.e. as found in DNe during outburst and in novalikes.)

DNOs have periods in the ∼5-40 s range, usually with an oscillation amplitude of <1% in the optical. They exhibit a characteristic period-luminosity relationship, i.e. the minimum period corresponds to the maximum $\dot{m}_{\rm acc}$ during the DN outburst, and the period increases during the after-outburst decline [20]. The value of Q is usually between 10^3 and 10^7 for DNOs. The period sometimes exhibits small jumps (∼0.01% of the period value), and 2 DNO periods are sometimes observed simultaneously [11]. DNOs have also been observed in the extreme ultraviolet and in soft X-rays, with amplitudes even up to 100% (e.g. [21]). The amplitude of the oscillation can be variable on time-scales of hours, and it can disappear and reappear.

The periodicities classified as lpDNOs are similar, but have periods typically ∼4 times longer than those of DNOs [22]. They are also observed only in CVs with high $\dot{m}_{\rm acc}$, but without the strong period-luminosity relationship of DNOs, and with slightly larger amplitudes. In cases where DNOs and lpDNOs are observed simultaneously, their amplitude and phase modulations are independent.

Still another type of oscillation is referred to as "quasi-periodic oscillations" (QPOs). Their periods and modulation amplitudes are much larger than those of DNOs, and they are less coherent: typically, $5 < Q < 20$. QPOs have been observed in CVs with high $\dot{m}_{\rm acc}$, but also in DNe during quiescence, and they are not dependent on the simultaneous presence of DNOs. However, in cases where QPOs do occur simultaneously with DNOs, it is found that $P_{\rm QPO}/P_{\rm DNO} \sim 15$, and the QPO is then referred to as a "DNO-related QPO" [22]. In several systems with "double DNOs", the QPO is the beat period of the double DNOs.

The most favoured interpretation for the rich variety of DNOs in CVs is that they originate close to the surface of a WD with a magnetic field too small to enable rigid body rotation by the core and exterior region, but strong enough to control accretion close to its surface.

The rotation period of the WD in DQ Her was studied by [19], who argued that the observed clock-like stability in P_* in intermediate polars must be due to rigid-body rotation. He proposed the WD magnetic field as the mechanism coupling the stable clock of the core to the exterior regions. The magnetic field that is necessary to transmit an observed acceleration $\dot{\Omega}_*$ from the outer regions to the core, or the other way around, is given by comparing the Maxwell and mechanical stresses:

$$\frac{B_r B_\phi}{4\pi} \approx \rho_{\rm wd}\, \dot{\Omega}_* R^2 \ , \tag{4.1}$$

where B_r and B_ϕ are the radial and azimuthal components of the internal magnetic field. By estimating $R \sim 10^9$ cm and a density of $\rho_{\rm wd} \sim 10^6$ g cm^{-3} (assuming that a substantial portion of the deep interior is still in fluid form and not yet crystalline), together with $\dot{\Omega}_* \approx 10^{-15}$ s^{-2} measured for DQ Her, $B_r B_\phi \sim 10^{10}$ G^2 was obtained, yielding a minimum field strength of $B_r \sim B_\phi \sim 10^5$ G.

A magnetic field weaker than this will not be able to couple the accretion torque to the interior, and this will allow the accumulation of an equatorial belt rotating rapidly at the local Keplerian

velocity. *HST* observations of dwarf novae have already provided direct evidence of the existence of a hot, rapidly rotating belt around a WD in relatively slow rotation [23, 24, 25, 26, 27]. Instead of the period of the equatorial belt being exactly equal to the local Keplerian period, its inertia may cause it to have a somewhat longer period than this [28]. This concept was initially suggested by [29], and was developed by [28] and [15] into a low-inertia magnetic accretor (LIMA) model.

In terms of the LIMA model, the mass contained in the equatorial belt is probably $<10^{-10}$ $M_{\odot}$, resulting in a much lower inertia than the WD as a whole. The period-luminosity relationship can be explained by the inner radius of the disc moving farther inward as $\dot{m}_{\rm acc}$ increases, yielding a shorter Keplerian period for the equatorial belt (spin-up). As $\dot{m}_{\rm acc}$ decreases in the final stages of the outburst, the inner disc boundary moves outward quickly, resulting in a fast outward centrifugal acceleration of the wound-up belt. Gas is now propellered outwards from the belt, removing angular momentum and thus rapidly spinning down the belt. The result is an equatorial belt with a longer Keplerian period and larger outer radius.

Magnetic field lines connecting the belt and the inner disc will be wound up, until reconnection occurs after differential rotation of $\sim 2\pi$, relieving the tension in the field lines (see [15] and references therein). The observed DNO period "jumps" superimposed on the more gradual variability are too rapid to also be explained by the spin-up and spin-down of the belt. Latitudinal variations in rotational period may be present in the belt, with the period increasing at higher latitudes towards P_* of the underlying primary. MHD turbulence caused by reconnection events may cause "accretion curtains", from which gas can be fed through accretion arcs at different latitudes. This could explain the discontinuous jumps in the period. In a practical sense, many accretion arcs would usually be involved simultaneously, and the actual detection of DNOs may only be because of the coincidental domination of one or two of the arcs.

The double DNO periods and the often associated DNO-related QPO period that are related as beat periods, can be explained if the shorter DNO is associated with the equatorial belt and the QPO with a structure such as a thickening in the disc (e.g. at the accretion stream impact) revolving around the primary in a prograde direction. The longer DNO is then caused by the reprocessing of the short DNO beam by the QPO structure, and essentially represents a beat between the two.

This class of CVs can thus be considered as an extension of intermediate polars to weaker magnetic fields. The lpDNOs are also thought to be associated with such systems, but are found to have periods of approximately one half of P_*. It was suggested that this connects the lpDNOs directly to the WD spin period, with the factor of 2 being due to magnetically channelled two-pole accretion onto the WD [11]. Because $P_{\rm lpDNO} \sim 4P_{\rm DNO}$, this implies that $P_* \sim 8P_{\rm DNO}$.

5. The modified LIMA model for CAL 83

With its slightly lower Q-value, $P(\sim 67$ s) in CAL 83 exhibits variability that is somewhat more rapid, and also a period that is slightly longer, than what is typically observed in DNOs. However, the general characteristics of $P(\sim 67$ s) are remarkably similar to those of DNOs, and interpreting $P(\sim 67$ s) within the framework of an adapted LIMA model is very interesting.

$P(\sim 67$ s) might originate in a similar equatorial region around the WD. The radius of a cold WD with a mass of 1.3 $M_{\odot}$ is $R_{\rm wd} = 4.0 \times 10^8$ cm [30, 31]. The photospheric radius of 7×10^8 cm is a factor of $\sim$1.8 times larger than this [7], indicating that the WD in CAL 83 has a

swollen atmosphere. The value of $\sim 7\times10^8$ cm can be taken as an approximate outer limit for the equatorial belt. The Keplerian radius corresponding to a 67 s period is 2.7×10^9 cm, while the Keplerian period at $\sim 7\times10^8$ cm is significantly lower, i.e. $\sim$9 s. A belt with rotation period $\sim$67 s at $\sim 7\times10^8$ cm thus rotates more slowly than the local Keplerian velocity, probably due to its coupling to a WD core with an even longer rotation period. For the existence of such a belt with larger angular velocity than the WD, the magnetic field of the WD is perhaps too weak to rigidly couple this region to its core.

Various observational properties of CAL 83 suggest that $\dot{m}_{\rm acc} \sim 10^{-7}$ M$_\odot$ yr^{-1} represents a realistic order-of-magnitude estimate for the accretion rate. Furthermore, the cylindrical Alfvén radius $R_{\rm M}$ describes the radial position inside of which the magnetic pressure will dominate the ram and gas pressure of the accreting material (e.g. [32, p. 160]):

$$R_{\rm M} \sim 10^8 \left(\frac{B_1}{10^5\ {\rm G}}\right)^{4/7} \left(\frac{R_1}{4.0\times10^8\ {\rm cm}}\right)^{12/7} \left(\frac{M_1}{1.3{\rm M}_\odot}\right)^{-1/7} \left(\frac{\dot{m}_{\rm acc}}{10^{-7}\ {\rm M}_\odot\ {\rm yr}^{-1}}\right)^{-2/7} {\rm cm}\ . \quad (5.1)$$

The potential spin-up rate $\dot{\Omega}_*$ of the WD due to accretion torques is dependent on $R_{\rm M}$ and can be obtained with (e.g. [32, p. 163])

$$\dot{\Omega}_* \sim\ 2\times10^{-15} \left(\frac{\dot{m}_{\rm acc}}{10^{-7}\ {\rm M}_\odot\ {\rm yr}^{-1}}\right) \left(\frac{M_1}{1.3\ {\rm M}_\odot}\right)^{1/2} \left(\frac{R_{\rm M}}{10^8\ {\rm cm}}\right)^{1/2} \left(\frac{I}{4\times10^{50}\ {\rm g\ cm}^2}\right)^{-1}\ {\rm s}^{-2}\ , \quad (5.2)$$

where I is the moment of inertia of the WD. An upper limit to the magnetic field strength of the WD in CAL 83 can be calculated with Eq. (4.1). An estimate of the potential spin-up rate $\dot{\Omega}_*$ due to accretion torques first needs to be obtained. From Eq. (5.1) and (5.2), one can see that the value of $\dot{\Omega}_*$ is proportional to B_1 to the power $2/7$ (through its dependence on $R_{\rm M}$), and therefore does not change too drastically with large changes in magnetic field. The value of $\dot{\Omega}_*$ changes by only one order of magnitude from 10^{-15} s^{-2} to 10^{-14} s^{-2} when varying the dipole field strength of the primary over the wide range from $B_1 \sim 7\times10^3$ G to $\sim 3\times10^7$ G.

Assuming $\rho_{\rm wd} \sim 10^6$ g cm^{-3}, the upper limit for the product of the interior magnetic field components to avoid rigid rotation according to Eq. (4.1), is

$$B_r B_\phi \approx 6\times10^9 \left(\frac{\rho_{\rm wd}}{10^6\ {\rm g\ cm}^{-3}}\right) \left(\frac{\dot{\Omega}_*}{10^{-15}\ {\rm s}^{-2}}\right) \left(\frac{R}{7\times10^8\ {\rm cm}}\right)^2\ {\rm G}^2\ . \quad (5.3)$$

Approximating the two components as being equal, and adopting $\dot{\Omega}_* \sim 10^{-15}$ s^{-2}, one obtains $B_r \sim B_\phi \lesssim 8\times10^4$ G, while for $\dot{\Omega}_* \sim 10^{-14}$ s^{-2}, the upper limit is $B_r \sim B_\phi \lesssim 2\times10^5$ G. In turn, the interior field strengths can be considered as an upper limit to the strength of the surface field B_1. Therefore, as an order of magnitude estimate, $B_1 \lesssim 10^5$ G is required to allow the existence of a non-corotating belt structure at $R \sim 7\times10^8$ cm.

We will now investigate the possibility that the modulations in $P(\sim 67$ s) may arise from the spin-up and spin-down of the equatorial belt. By investigating the dynamic periodograms and considering the most rapid observed decrease in $P(\sim 67$ s), the maximum spin-up rate of the belt was estimated to be $\dot{\Omega}_{\rm b} \sim 1.8\times10^{-6}$ s^{-2}. The specific angular momentum of the belt magnetically

linked to the WD is estimated by $Rv_{\mathrm{b},\phi}$, where $v_{\mathrm{b},\phi} = 2\pi R/P_{\mathrm{b}}$ is its azimuthal velocity. The spin-up rate $\dot{\Omega}_{\mathrm{b}}$ of the belt can thus be expressed as

$$\dot{\Omega}_{\mathrm{b}} = \dot{m}_{\mathrm{acc}} \left(\frac{2\pi R^2}{P_{\mathrm{b}}} \right) I_{\mathrm{b}}^{-1} \, , \tag{5.4}$$

or, solving for the moment of inertia I_{b} of the belt, one obtains

$$I_{\mathrm{b}} \sim 1.6 \times 10^{41} \left(\frac{\dot{m}_{\mathrm{acc}}}{10^{-7}\ \mathrm{M}_{\odot}\ \mathrm{yr}^{-1}} \right) \left(\frac{\dot{\Omega}_{\mathrm{b}}}{1.8 \times 10^{-6}\ \mathrm{s}^{-2}} \right)^{-1} \left(\frac{R}{7.0 \times 10^{8}\ \mathrm{cm}} \right)^{2} \left(\frac{P_{\mathrm{b}}}{67\ \mathrm{s}} \right)^{-1} \mathrm{g\ cm}^2 \, , \tag{5.5}$$

which is almost 10 orders of magnitude smaller than that of the WD. This represents a maximum value for the inertia if the observed $\dot{\Omega}_{\mathrm{b}}$ is to be explained by the spin-up of the belt. One can now proceed to estimate the mass of the belt. It will be assumed that the geometry of the belt can be described as an annular cylinder around the WD, with central axis perpendicular to the orbital plane. The outer radius R_{b2} of the belt will be taken as approximately equal to the photospheric radius of the envelope, i.e. $\sim 7 \times 10^8$ cm. The inner radius R_{b1} of the cylinder has a lower limit of $R_{\mathrm{wd}} \sim 4 \times 10^8$ cm, although R_{b1} is probably larger than this. The moment of inertia is then given by (e.g. [33, p. 253])

$$I_{\mathrm{b}} = \frac{1}{2} m_{\mathrm{b}} \left(R_{\mathrm{b1}}^2 + R_{\mathrm{b2}}^2 \right) \, , \tag{5.6}$$

where m_{b} is the mass of the belt, and adopting the radii above yields $m_{\mathrm{b}} = 2.5 \times 10^{-10}\ \mathrm{M}_{\odot}$. The critical envelope mass required for the ignition of nuclear burning is given by ([34] and references therein)

$$\log \left(\frac{m_{\mathrm{env}}^{\mathrm{crit}}}{\mathrm{M}_{\odot}} \right) \approx \ -2.862 + 1.542 \left(\frac{M_{\mathrm{wd}}}{\mathrm{M}_{\odot}} \right)^{-1.436} \ln \left(1.429 - \frac{M_{\mathrm{wd}}}{\mathrm{M}_{\odot}} \right) - 0.197 \left[\log \left(\frac{\dot{m}_{\mathrm{acc}}}{\mathrm{M}_{\odot}\ \mathrm{yr}^{-1}} \right) + 10 \right]^{1.484} \, , \tag{5.7}$$

yielding $m_{\mathrm{env}}^{\mathrm{crit}} \sim 9 \times 10^{-7}\ \mathrm{M}_{\odot}$ for a 1.3 $\mathrm{M}_{\odot}$ WD accreting at $\sim 10^{-7}\ \mathrm{M}_{\odot}\ \mathrm{yr}^{-1}$, which can be considered as a lower limit for the envelope mass for nuclear burning to occur. Therefore, if $m_{\mathrm{b}} = 2.5 \times 10^{-10}\ \mathrm{M}_{\odot}$ the equatorial belt represents only a small fraction of the total envelope mass.

Considering the extended, "fuzzy" nature of the WD envelope in SSSs, cloaking the nuclear burning shell, this scenario seems quite plausible. An equatorial belt at the envelope-disc boundary may have a rotational period of $\sim$67 s as described above, while accreted layers closer to the WD may be rotating with slightly longer periods, yielding differential rotation between these weakly coupled layers at different radial distances. In such a case it is more likely that the inner radius of the belt is significantly larger than the WD radius. Increasing R_{b1} up to almost $R_{\mathrm{b2}} = 7 \times 10^8$ cm (implying a thin shell at this radius) yields $m_{\mathrm{b}} = 1.6 \times 10^{-10}\ \mathrm{M}_{\odot}$, i.e. the presumed thickness of the shell does not change the resulting mass significantly.

The ram pressure dominated flow will result in a significant winding up of the WD magnetic field frozen into the belt plasma. This will result in the generation of a significant toroidal external field. Assuming that the rotation period of the WD is substantially longer than that of the belt, the

belt will carry the footpoints of the field lines around its orbit, stretching the field lines and creating a substantial toroidal field component $B_{\mathrm{b},\phi}$ in the vicinity of the belt (e.g. [35]). It was shown by [15] that the toroidal field generated by the belt is given by

$$B_{\mathrm{b},\phi} \sim 2\times10^{5}\left(\frac{B_r}{10^5\ \mathrm{G}}\right)^{1/2}\left(\frac{P_{\mathrm{b}}}{67\ \mathrm{s}}\right)^{-1/2}\left(\frac{m_{\mathrm{b}}}{2\times10^{-10}\ \mathrm{M}_{\odot}}\right)^{1/4}\times$$
$$\left(\frac{T}{5.5\times10^{5}\ \mathrm{K}}\right)^{1/4}\left(\frac{x}{0.1}\right)^{-1/4}\left(\frac{y}{0.01}\right)^{-1/4}\left(\frac{M_1}{1.3\ \mathrm{M}_{\odot}}\right)^{-1/4}\ \mathrm{G}\,. \qquad (5.8)$$

The height of the belt (in the direction perpendicular to the orbital plane) is given by xR_1. The quantity yg represents the effective gravity in the belt, where g is the surface gravity of the WD. The approximations $x\sim0.1$ and $y\sim0.01$ of [15] were also used here. Adopting $T=550000$ K according to the fits of [7], as well as $m_{\mathrm{b}}\sim2\times10^{-10}$ M$_{\odot}$, yields a toroidal field of $\sim2\times10^5$ G for an original poloidal field of 10^5 G, which indicates a significant enhancement. It has been shown ([36], e.g. [37]) that when the stretched toroidal field exceeds the poloidal WD field by up to 10 times, the field will become unstable to magnetic reconnection.

As the toroidal component $B_{\mathrm{b},\phi}$ of the magnetic field grows, the amplified field pressure starts to dominate the fluid pressure therefore erupting as prominences between the rotating compact object and the adjacent envelope which constitutes the inner edge of the disc. This configuration will be unstable to reconnection (see [38, Chapter 6]) and may result in the ejection of magnetized "bubbles" which will be centrifugally expelled from the system (see Fig. 2). These magnetic bubbles carry a significant amount of angular momentum, which if lost from the system, may provide a very efficient angular momentum drain that can sustain the required high mass transfer to drive nuclear burning on the surface of the accreting white dwarf.

As an alternative to spin-up and spin-down of the belt, the rapid changes in the value of $P(\sim67\ \mathrm{s})$ within a single observation may be caused by the same mechanism proposed to explain the discontinuous jumps in the DNOs: the channelling of the accretion flow onto different accretion arcs in the belt as a result of magnetic reconnection. In such a case, the disappearance and reappearance of the period on time-scales of hours may be due to the accretion being channelled dominantly onto latitudes with the same period at some epochs (i.e. a well-defined period is observable), with accretion onto a wide range of latitudes with different periods at other epochs (i.e. a well-defined oscillation peak is not observable).

If spin-up and spin-down is not the primary cause of the period modulations, then the upper limit imposed on the inertia earlier in this section would not be so strict, and a larger fraction of the envelope mass could form part of the equatorial belt. However, the variation in $P(\sim67\ \mathrm{s})$ is probably caused by a combination of spin-up/spin-down and magnetic reconnection mechanisms.

Comparing the mean period and X-ray luminosity from observation to observation, marginal evidence has been found that $P(\sim67\ \mathrm{s})$ is on average somewhat shorter when the X-ray luminosity (and the corresponding temperature) is higher. This could simply be due to the fact that higher count rates and temperatures indicate a slightly more contracted photospheric radius, with the belt at the envelope-disc boundary subsequently being at a slightly smaller radius with a smaller corresponding period. However, it is noted that the modulation in $P(\sim67\ \mathrm{s})$ from observation to observation over the years is not any larger than its modulation on time-scales of hours.

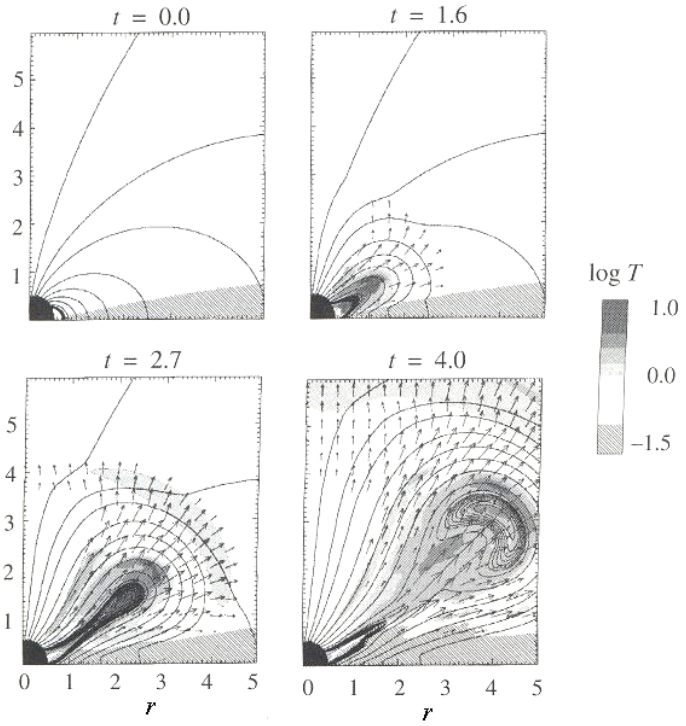

Figure 2: Centrifugal ejection of magnetized plasma bubbles from accretion discs. Adopted from [38].

If $P(\sim 67$ s) observed is analogous to an "ordinary" DNO in a DN, one could hypothetically expect the inherent presence of additional oscillations close $P_{\rm lpDNO} = 4 \times 67$ s $= 268$ s (3.7 mHz) and $P_* = 8 \times 67$ s $= 536$ s (1.9 mHz) in the lightcurves (although the presence of a DNO does not necessarily mean that a lpDNO and/or WD rotation period should also be detectable). In the CAL 83 X-ray periodograms, the only peak close to either 3.7 or 1.9 mHz that has a >99.73% significance level, is one at ∼1.7 mHz (580 s) in observation 0506530501. None of the other observations contained an apparent peak at ∼1.9 mHz. In the second exposure of observation 0123510101B, and especially 0500860201 and 0506531201, a weak peak is visible approximately at 3.7 mHz, although below the >99.73% significance level. Although we can thus not confirm or exclude the presence of consistent periodicities at $P_{\rm lpDNO} = 4 \times 67$ s and $2 \times P_{\rm lpDNO}$, this is something that could be investigated in more detail using new X-ray data.

Optical and ultraviolet spectra of CAL 83 indicate that an accretion disc is present around the WD. As illustrated in this section, the presence and properties of such an accretion disc play a key role in the interpretation of the X-ray modulations on time-scales from 67 s to days or years. Although the interaction of the inner disc with the WD envelope may be observed in soft X-rays, the regions farther out in the disc emit in the optical waveband. In the next section, a series of optical lightcurves of CAL 83 is presented.

6. SHOC lightcurves

Optical lightcurves of CAL 83 were obtained with the Sutherland High-speed Optical Camera

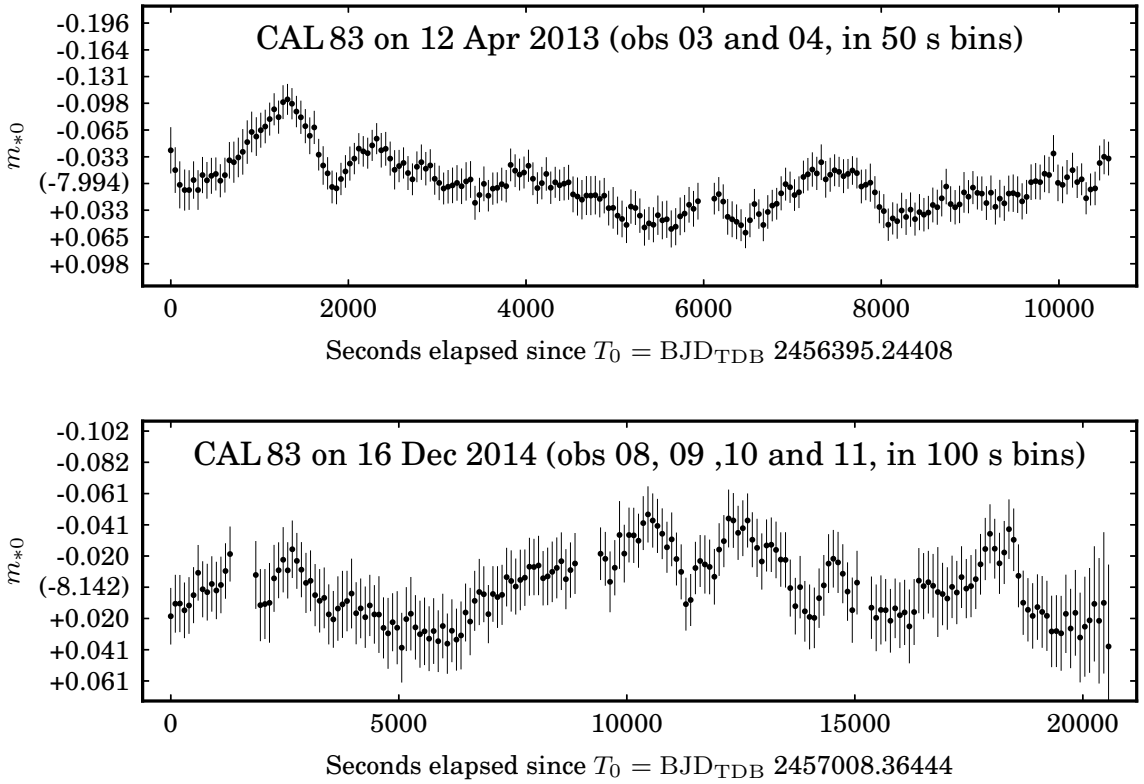

Figure 3: Two of the SHOC lightcurves of CAL 83, after differential correction. The horizontal axis indicates the seconds elapsed since the first measurement in the observation. On the vertical axis, the mean corrected instrumental magnitude is given in parentheses, with the other markings indicating integer multiples of the standard deviation of the lightcurve, referred to the mean value.

(SHOC) on the SAAO 1.9-m Telescope, using a clear filter, on 8 nights during April 2013 and December 2014 (see [16, Chapter 6] for details). Standard IRAF procedures were used to reduce the data, after which differential corrections using 4 comparison stars was applied, utilizing a method largely based on the one described by [39]. The two longest lightcurves are shown in Fig. 3, i.e. those obtained on the nights of 12 Apr 2013 and 16 Dec 2014.

The exposure times for the SHOC datasets were 10 s or shorter, therefore all the lightcurves had adequate time resolution to allow for the detection of a 67 s periodicity. However, no discernible power peak around 67 s was observed in the periodograms of these lightcurves. However, smooth modulations that can almost be described as "hump"-like structures are present in all the lightcurves, i.e. a smooth rise and decline lasting for $\gtrsim$1000 s, with an amplitude of up to $\sim$0.1 mag. In Fig. 3, these structures can be seen to commence at $\sim$200 s after T_0 and again at $\sim$6500 s in the 12 Apr 2013 lightcurve, and at $\sim$2000 s, $\sim$9500 s, $\sim$11500 s, $\sim$14000 s, and $\sim$17500 s after T_0 in the 16 Dec 2014 observation. Similar structures with slightly smaller amplitudes and periods also seem to be present in some of the lightcurves.

Although these rise-and-decline patterns seem to repeat themselves, they are not strictly periodic; they can be described as quasi-periodic at most. In the 16 Dec 2014 lightcurve, a slower rise and decline starting at $T_0 \sim 6000$ s and lasting for approximately 10000 s, is also evident. No

deviation of more than ∼0.1 mag from the mean was observed within a single night. The maximum change in the mean magnitude from one night to the next is also only ∼0.1 mag.

Although the known orbital modulation of ∼1 d in the optical should be present in the SHOC lightcurves, the timespan of even the longest of the SHOC observation is still significantly shorter than the orbital period, therefore it is evident that variability on shorter time-scales is superimposed on the presumed underlying orbital modulation. These modulations are expected to originate in the accretion disc, which is the dominant source of optical emission in SSSs. It can be shown that the time-scales of these modulations are compatible with Keplerian periods in the inner regions of the accretion disc, possibly of turbulent eddies that dissipate after one or two orbits. However, the extended rim of the accretion disc is expected to be the dominant source of (reprocessed) optical emission from the system [40, 41]. Therefore, the optical modulations may also be related to small changes in the structure of the rim itself, or perhaps the movement of blobs inside the rim.

As explained in §4, QPOs (quasi-periodic oscillations) occurring simultaneously with DNOs often exhibit the period relation $P_{\rm QPO}/P_{\rm DNO} \sim 15$. Adopting $P_{\rm DNO} \sim 67$ s leads to a period of $P_{\rm QPO} \sim 15 \times 67$ s ~ 1000 s for a potential DNO-related QPO in the system. It is interesting to note that this predicted time-scale is of the same order as the quasi-periodic modulations that have been observed in the SHOC lightcurves. $P(\sim 67$ s) is observed in X-rays because it originates in a region close to the WD, where high temperatures are found due to the surface nuclear burning. The quasi-periodic modulations are expected to occur farther out in the accretion disc where temperatures are lower, rendering these regions of the disc visible in the optical waveband.

7. The LIMA model and possible transient non-thermal emission

It has been mentioned earlier that the LIMA model applied to CAL 83 essentially implies the formation of tightly wound up toroidal magnetic fields as a result of the differential rotation between the WD and the envelope of gas that constitute the inner edge of the disc. As mentioned earlier, this will result in the formation of magnetic prominences when the field pressure exceeds the ambient plasma pressure, which will reconnect as a result of a topological reconfiguration of the magnetic field as it seeks a more stable configuration. Magnetic reconnection may be a very efficient process to convert magnetic energy into accelerated particles [42], that may manifest in non-thermal emission through synchrotron, non-thermal bremmstrahlung and inverse Compton radiation. Utilizing Faraday's induction law, the work done per unit charge (*emf*) in a single orbit (e.g. [37] and references therein) is

$$emf = \frac{\pi B R_{\rm L} v_{\rm m}}{c} \, , \tag{7.1}$$

where $R_{\rm L}$ represent the Larmor radius and $v_{\rm m} \sim 0.1 c_{\rm s}$ the typical merging speed of the magnetic field in the plasma expressed in terms of the local sound speed (e.g. [37] for a discussion). The electric field in the merging region (MR) is then of the order of

$$E_{\rm MR} = \frac{\pi B v_{\rm m}}{c} \, . \tag{7.2}$$

It can be shown that magnetic reconnection in fields of the order of $B_\phi \sim 10B_r \sim 10^6$ G can readily produce electric fields of the order of

$$E_{\rm MR} \sim 3000 \left(\frac{B_\phi}{10^6\ {\rm G}}\right)\left(\frac{v_{\rm m}}{0.1\,c_{\rm s}}\right) {\rm Volt\ cm^{-1}}\ . \tag{7.3}$$

This implies that particles can readily be accelerated to energies of the order of $\varepsilon_{\rm e} >$ few MeV over length scales of only a few kilometres, which is short compared to the global length scales of the magnetic flux tubes. This may provide very interesting possibilities for possible non-thermal transient synchrotron emission that can be searched for with the SKA precursor *MeerKAT* that will become operational soon, as well as in X-ray and soft gamma-ray energy bands.

8. Conclusion

It has been shown that the properties of the ∼67 s X-ray periodicity in CAL 83 ($P(\sim 67$ s)) are remarkably similar to those of the DNOs observed in DNe during outburst. The existing low inertia magnetic accretor (LIMA) model for DNOs has been applied to $P(\sim 67$ s), and through a broad quantitative analysis it has been shown to provide a very promising physical explanation for the variable nature of $P(\sim 67$ s). Within the LIMA model, the periodicity originates in an equatorial belt around a weakly magnetized WD. The belt is not in rigid corotation with the WD core, allowing it to rotate faster than the WD itself. The period variations are related to a combination of spin-up and spin-down of the belt, and the channelling of the accretion stream through different accretion arcs. SHOC optical lightcurves of CAL 83 exhibit quasi-periodic modulations with periods of the order of 1000 s, which also fit well within the LIMA framework. The generation of a significant toroidal magnetic field by the winding up of field lines in the rotating belt would lead to magnetic reconnection events, which could result in the conversion of magnetic energy into the kinetic energy of accelerated particles. This process is expected to yield transient non-thermal emission events from radio to possibly gamma-ray energies.

Acknowledgments

The authors would like to thank the conference organisers for the opportunity to present this work, as well as an anonymous referee for the constructive feedback. The financial assistance of the South African Square Kilometre Array Project towards this research is hereby acknowledged. Opinions expressed and conclusions arrived at, are those of the author and are not necessarily to be attributed to the NRF.

References

[1] K. S. Long, D. J. Helfand, and D. A. Grabelsky, *A soft X-ray study of the Large Magellanic Cloud*, *ApJ* **248** (1981) 925–944.

[2] F. D. Seward and M. Mitchell, *X-ray survey of the Small Magellanic Cloud*, *ApJ* **243** (1981) 736–743.

[3] J. Trümper, G. Hasinger, B. Aschenbach, H. Bräuninger, U. G. Briel, W. Burkert, H. Fink, E. Pfeffermann, W. Pietsch, P. Predehl, J. H. M. M. Schmitt, W. Voges, U. Zimmermann, and K. Beuermann, *X-ray survey of the Large Magellanic Cloud by ROSAT*, *Nature* **349** (1991) 579–583.

[4] E. P. J. Van den Heuvel, D. Bhattacharya, K. Nomoto, and S. A. Rappaport, *Accreting white dwarf models for CAL 83, CAL 87 and other ultrasoft X-ray sources in the LMC*, *A&A* **262** (1992) 97–105.

[5] T. Brown, F. Cordova, R. Ciardullo, R. Thompson, and H. Bond, *Einstein observations of ultrasoft X-ray sources in the Magellanic Clouds*, *ApJ* **422** (1994) 118–125.

[6] A. F. Rajoelimanana, P. A. Charles, P. J. Meintjes, A. Odendaal, and A. Udalski, *Optical and X-ray properties of CAL 83 - I. Quasi-periodic optical and supersoft variability*, *MNRAS* **432** (2013) 2886–2894.

[7] T. Lanz, G. A. Telis, M. Audard, F. Paerels, A. P. Rasmussen, and I. Hubeny, *Non-LTE Model Atmosphere Analysis of the Large Magellanic Cloud Supersoft X-Ray Source CAL 83*, *ApJ* **619** (2005) 517–526.

[8] A. Odendaal and P. J. Meintjes, *CAL 83 — The Prototypical Close Binary Supersoft X-ray Source in the LMC: A Short Review*, *Conference Papers in Science* **in press** (2015).

[9] A. Odendaal and P. J. Meintjes, *Multiwavelength variability in CAL 83*, in *High Energy Astrophysics in Southern Africa 2014: A multi-frequency perspective of new frontiers in High Energy Astrophysics in Southern Africa. Mem. S.A.It. 86(1)*, pp. 102–107, 2015.

[10] S. Scaringi, *A physical model for the flickering variability in cataclysmic variables*, *MNRAS* **438** (2014) 1233–1241.

[11] B. Warner, *Rapid Oscillations in Cataclysmic Variables*, *PASP* **116** (2004) 115–132.

[12] B. Warner and P. A. Woudt, *QPOs in CVs: An executive summary*, in *American Institute of Physics Conference Series* (M. Axelsson, ed.), vol. 1054 of *American Institute of Physics Conference Series*, pp. 101–110, 2008.

[13] A. Odendaal, P. J. Meintjes, P. A. Charles, and A. F. Rajoelimanana, *Optical and X-ray properties of CAL 83 - II. An X-ray pulsation at ∼67 s*, *MNRAS* **437** (2014) 2948–2956.

[14] J.-U. Ness, A. P. Beardmore, J. P. Osborne, E. Kuulkers, M. Henze, A. L. Piro, J. J. Drake, A. Dobrotka, G. Schwarz, S. Starrfield, P. Kretschmar, M. Hirsch, and J. Wilms, *Short-period X-ray oscillations in super-soft novae and persistent super-soft sources*, *A&A* **578** (2015) A39.

[15] B. Warner and P. A. Woudt, *Dwarf nova oscillations and quasi-periodic oscillations in cataclysmic variables - II. A low-inertia magnetic accretor model*, *MNRAS* **335** (2002) 84–98.

[16] A. Odendaal, *The Multiwavelength Properties of a Sample of Magellanic Cloud and Galactic Supersoft X-ray Binaries*. PhD thesis, University of the Free State, Bloemfontein, 2015.

[17] J. Greiner and R. Di Stefano, *X-ray off states and optical variability in CAL 83*, *A&A* **387** (2002) 944–954.

[18] P. C. Schmidtke and A. P. Cowley, *X-Ray Pulsations in the Supersoft X-Ray Binary CAL 83*, *AJ* **131** (2006) 600–602.

[19] J. I. Katz, *The structure of DQ Herculis.*, *ApJ* **200** (1975) 298–305.

[20] J. Patterson, *Rapid oscillations in cataclysmic variables. VI - Periodicities in erupting dwarf novae*, *ApJS* **45** (1981) 517–539.

[21] M. H. Jones and M. G. Watson, *The EXOSAT observations of SS Cygni*, *MNRAS* **257** (1992) 633–649.

[22] B. Warner, P. A. Woudt, and M. L. Pretorius, *Dwarf nova oscillations and quasi-periodic oscillations in cataclysmic variables - III. A new kind of dwarf nova oscillation, and further examples of the similarities to X-ray binaries*, *MNRAS* **344** (2003) 1193–1209.

[23] E. M. Sion, F.-H. Cheng, M. Huang, I. Hubeny, and P. Szkody, *The Cooling White Dwarf in VW Hydri after Normal Outburst and Superoutburst: HST Evidence of a Sustained Accretion Belt*, *ApJ* **471** (1996) L41.

[24] B. T. Gänsicke and K. Beuermann, *The cooling of the white dwarf in VW Hyi.*, *A&A* **309** (1996) L47–L50.

[25] F. H. Cheng, E. M. Sion, K. Horne, I. Hubeny, M. Huang, and S. D. Vrtilek, *HST synthetic spectral analysis of U GEM in early and late quiescence: A heated white dwarf and accretion belt?*, *AJ* **114** (1997) 1165.

[26] P. Szkody, D. W. Hoard, E. M. Sion, S. B. Howell, F. H. Cheng, and W. M. Sparks, *Ultraviolet and Optical Spectroscopy Of AL Comae 1 Year After Superoutburst*, *ApJ* **497** (1998) 928–934.

[27] E. M. Sion and J. Urban, *The Extraordinary Cataclysmic Binary RU Pegasi: The Hottest White Dwarf in a Dwarf Nova?*, *ApJ* **572** (2002) 456–460.

[28] B. Warner, *DQ Herculis Stars and Dwarf Nova Oscillations*, in *Magnetic Cataclysmic Variables* (D. A. H. Buckley and B. Warner, eds.), vol. 85 of *Astronomical Society of the Pacific Conference Series*, p. 343, 1995.

[29] B. Paczyński, *Phenomenological Model of U Geminorum*, in *Nonstationary Evolution of Close Binaries* (A. N. Zytkow, ed.), p. 89, 1978.

[30] T. Hamada and E. E. Salpeter, *Models for Zero-Temperature Stars.*, *ApJ* **134** (1961) 683.

[31] M. Eracleous and K. Horne, *The Speedy Magnetic Propeller in the Cataclysmic Variable AE Aquarii*, *ApJ* **471** (1996) 427.

[32] J. Frank, A. R. King, and D. Raine, *Accretion Power in Astrophysics*. Cambridge University Press, Cambridge, 3 ed., 2002.

[33] D. Halliday, R. Resnick, and J. Walker, *Fundamentals of physics*. Wiley international edition. Wiley, 2005.

[34] P. Kahabka and E. P. J. van den Heuvel, *Super Soft Sources*, ch. 11, pp. 461–474. Cambridge University Press, New York, 2006.

[35] J. J. Aly and J. Kuijpers, *Flaring interactions between accretion disk and neutron star magnetosphere*, *A&A* **227** (1990) 473–482.

[36] P. Ghosh and F. K. Lamb, *Plasma physics of accreting neutron stars*, in *NATO Advanced Science Institutes (ASI) Series C* (J. Ventura and D. Pines, eds.), vol. 344 of *NATO Advanced Science Institutes (ASI) Series C*, p. 363, 1991.

[37] P. J. Meintjes and O. C. de Jager, *Propeller spin-down and the non-thermal emission from AE Aquarii*, *MNRAS* **311** (2000) 611–620.

[38] E. Priest and T. Forbes, *Magnetic Reconnection: MHD Theory and Applications*. Cambridge University Press, 2000.

[39] M. E. Everett and S. B. Howell, *A Technique for Ultrahigh-Precision CCD Photometry*, *PASP* **113** (2001) 1428–1435.

[40] S. Schandl, E. Meyer-Hofmeister, and F. Meyer, *Visual light from the eclipsing supersoft X-ray source CAL 87.*, *A&A* **318** (1997) 73–80.

[41] E. Meyer-Hofmeister, S. Schandl, and F. Meyer, *The structure of the accretion disk rim in supersoft X-ray sources.*, *A&A* **321** (1997) 245–253.

[42] E. N. Parker, *The Acceleration of Particles to High Energy*, in *NATO Advanced Science Institutes (ASI) Series C* (G. Setti, ed.), vol. 28 of *NATO Advanced Science Institutes (ASI) Series C*, p. 137, 1976.